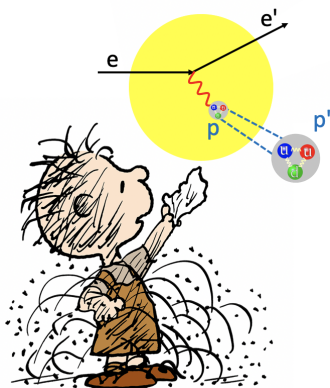


# Letter of Intent to PAC 50: Color Transparency in Dirty Kinematics

S. Li\*, J. Rittenhouse West  
Lawrence Berkeley National Laboratory,  
Berkeley, California 94720, USA

D.W. Higinbotham, H. Szumila-Vance  
Thomas Jefferson National Accelerator Facility,  
Newport News, Virginia 23606, USA

C. Yero  
Old Dominion University, Norfolk, VA 23529, USA



## Abstract

With the current highest beam energy at Jefferson Lab using traditional methods, we have exhausted our sensitivity for seeing the onset of proton color transparency (CT) in a nucleus in traditional electron scattering kinematics. A classic technique for dealing with such a problem is to look for ways to enhance the signal. In this spirit, we propose a CT measurement in dirty kinematics where final-state interactions (FSIs) and re-scatterings are known to be huge effects. By measuring in these kinematics as a function of increasing space-like 4-momentum transfer squared  $Q^2$ , we will have dramatically higher sensitivity to any possible CT signal than possible in the parallel kinematics of the traditional CT ( $e, e'p$ ) measurements at Jefferson Lab.

We propose to measure the  $d(e, e'p)n$  proton knockout cross sections for kinematics with known high FSIs and re-scattering effects to extract the proton nuclear transparency as a function of increasing  $Q^2$ . This allows us to construct the transparency ratio of the detected protons from the high momentum tail to those with low momentum as both the high and low regimes are characterized by different FSI effects. We will measure the transparency with high momentum transfer over the range of  $Q^2 = 8-15$  (GeV/c)<sup>2</sup>. We request a total of 95 days of beam time.

---

\*Contact Person: shujie1i@lbl.gov

# 1 Introduction

The strong force is well-described at low energies and long distances by the exchange of color-neutral mesons between nucleons while at high energies and short distances a perturbative QCD description with color-charged quark and gluonic degrees of freedom is valid. The boundary between these two regimes is a mystery, but each of them enables precise descriptions of nuclear interactions in their respective domains. While QCD is the theory of the strong interaction and the basis for nuclear phenomena, there are many missing links needed for it to directly describe matter in terms of nucleons and nuclei. The onset regime for color transparency in the proton, if discovered, is a direct link between QCD and nuclear physics.

## 1.1 Color Transparency

For exclusive processes at high momentum transfer, QCD predicts the phenomenon of color transparency (CT) [1] in which one can preferentially scatter off hadrons that have fluctuated into a point-like configuration (PLC), the quarks form an object of reduced transverse size, and the PLC exits the nucleus with no further interactions. A PLC implies that the external color fields of the hadron cancel (the object is color-neutral), thereby suppressing further gluonic interactions with the nuclear medium. The PLC is maintained for some period of time described by the expansion factor  $\tau$  (expansion time in the PLC rest frame). CT is uniquely predicted by QCD and exists at high momentum transfer. The momentum regime of the onset of CT is of interest because it sits at the transition between the low energy hadronic description and the high energy partonic description of nuclei.

The transparency variable,  $T$ , is defined as the cross section per nucleon for a process on a bound nucleon relative to that of a free nucleon such that  $T = \sigma_A / (A\sigma_0)$ . The onset of color transparency is experimentally measured as an increase in the transparency with increasing momentum transfer (or momentum transfer squared,  $Q^2$ , as is commonly used).

CT is relevant to QCD factorization theorems and the onset ( $Q^2$ ) of CT is where leading order perturbative QCD is applicable. Factorization theorems derived for deep inelastic exclusive processes are required for accessing Generalized Parton Distributions (GPDs) [2–5]. GPDs map the nucleon wave function and describe the transverse momentum and angular momentum carried by quarks in the proton [6, 7]. The full mapping of GPDs is the subject of significant experimental efforts in nuclear physics today. Furthermore, this suppression of final state interactions is essential to Bjorken scaling in the deep-inelastic regime at small  $x_B$  [8].

An important detail of CT is that the PLC must expand as it moves through the nucleus because it is not an eigenstate of the Hamiltonian. There are no precise calculations of the expansion time  $\tau$  or the expansion rate. Inside the nucleus the rate is time dilated to  $E/M/\tau$  (where  $E$  is the excitation energy of the PLC). One estimate of  $c\tau$  is given as 1 fm [9]. Previous estimates extracted  $\tau$  from the BNL ( $p, pp$ ) reactions assuming that the transparency rise was from CT. The same value of  $\tau$  was used to predict CT in ( $e, e'\pi$ ), ( $e, e'\rho$ ), and ( $e, e'p$ ). The  $\tau$  predictions are consistent with the meson production data but have been unsuccessful in predicting the onset of CT in protons. There is no strict reason that the expansion time should be the same for meson and baryons. If protons have a smaller  $\tau$  than mesons, the onset of CT is delayed to higher outgoing proton energy (proportional to  $Q^2$ ). At  $Q^2 = 20 \text{ GeV}/c^2$ ,  $\tau = 11 \text{ fm}^{-1}$  ( $1/\tau \approx 3 \times$  radius of  $^{12}\text{C}$ ). This indicates that up to  $Q^2 = 20 \text{ GeV}/c^2$ , there is motivation to measure the onset of CT in baryons to determine if PLC formation could be related to the observed EMC Effect [10]. In such models, the EMC effect is explained as a result of the suppression of PLCs in the bound nucleon wave function, which is emphasized when the bound nucleon is highly-virtual (states that are also dominated by short range correlated nucleon pairs) [11].

## 1.2 Previous CT measurements at intermediate energies

Measurements in the intermediate energy regime are of direct interest to the observation of the onset of CT. The onset of CT is favored to be observed at lower energy in mesons than baryons since only two quarks must come close together, and the quark-antiquark pair is more likely to form a PLC [12]. Pion production measurements at JLab reported evidence for the onset of CT [13] in the process  $e + A \rightarrow e + p + A^*$ . The results of the pion electroproduction experiment showed that both the energy and  $A$  dependence of the nuclear transparency deviate from conventional nuclear physics and are consistent with models that include CT. The results indicate that the energy scale for the onset of CT in mesons is  $\sim 1$  GeV.

A CLAS experiment studied  $\rho$ -meson production from nuclei, and the results also indicated an early onset of CT in mesons [14]. Previous  $\rho^0$  production experiments had shown that nuclear transparency also depends on the coherence length,  $l_c$ , which is the length scale over which the  $q\bar{q}$  states of mass  $M_{q\bar{q}}$  can propagate. The CLAS collaboration further measured the transparency for incoherent exclusive  $\rho^0$  electroproduction off carbon and iron relative to deuterium [14] using a 5 GeV electron beam. An increase of the transparency with  $Q^2$  for both C and Fe was observed. The rise in transparency was found to be consistent with predictions of CT by models [15, 16] which had accounted for the increase in transparency for pion electroproduction. The  $\pi$  and  $\rho$  electroproduction data set the energy range to be at a few GeV for the onset of CT in mesons.

While several experiments have observed a rise in the transparency for mesons, the observation of the onset of color transparency in baryons remains ambiguous. The focus of this proposal is to search for the onset of CT in baryons using deuterium.

## 1.3 CT in baryons at intermediate energies

The observed signal of the onset of CT in baryons remains ambiguous. The first attempt measured large angle  $A(p, pp)$  scattering at Brookhaven National Lab (BNL) [17–20]. These experiments measured the transparency as the quasi-elastic cross section from the nuclear target to the free  $pp$  elastic cross section. The results of these experiments indicated a rise in the transparency for outgoing proton momenta of 6–9.5 GeV/ $c$  consistent with models of CT. However, the transparency was observed to decrease at higher momenta between 9.5–14.4 GeV/ $c$ . This decrease is inconsistent with CT as a plateau after the onset is predicted for CT. The results of these experiments are not fully explained by anyone. The BNL experiments have an additional complication in that the incident proton suffers a reduction of flux in medium and must be included in any transparency calculation. Possible explanations include an elastic energy dependent cross section due to nuclear filtering from the Landshoff mechanism [21, 22] or excitation of charm resonances beyond the charm production threshold [23].

The  $(e, e'p)$  reaction is simpler to understand than the  $(p, pp)$  reaction as only the final state proton suffers a reduction of flux and needs to be considered in the measurement. The first experiments using an electron beam to measure CT were at SLAC [25, 27] followed up by experiments at JLab [24, 26]. In high  $Q^2$  quasielastic  $(e, e'p)$  scattering from nuclei, the electron scatters from a single proton, which has some associated Fermi motion [28]. In the plane wave impulse approximation (PWIA), the proton is ejected without final state interactions with the residual  $A - 1$  nucleons. The measured  $A(e, e'p)$  cross-section would be reduced compared to the PWIA prediction in the presence of final state interactions, where the proton can scatter both elastically and inelastically from the surrounding nucleons as it exits the nucleus. The deviations from the PWIA model measure the nuclear transparency. In complete CT, the final state interactions would vanish, and the nuclear transparency would plateau. This is in contrast to the conventional picture where the nuclear transparency is expected to follow the same energy dependence as the relatively energy-independent  $NN$  cross-section.

The combined results of searches for CT in the  $A(e, e'p)$  reaction are shown in Fig. 1. The results indicate that there is not significant rise up to  $Q^2 = 8$  GeV/ $c^2$ . If translating the  $A(p, pp)$  BNL

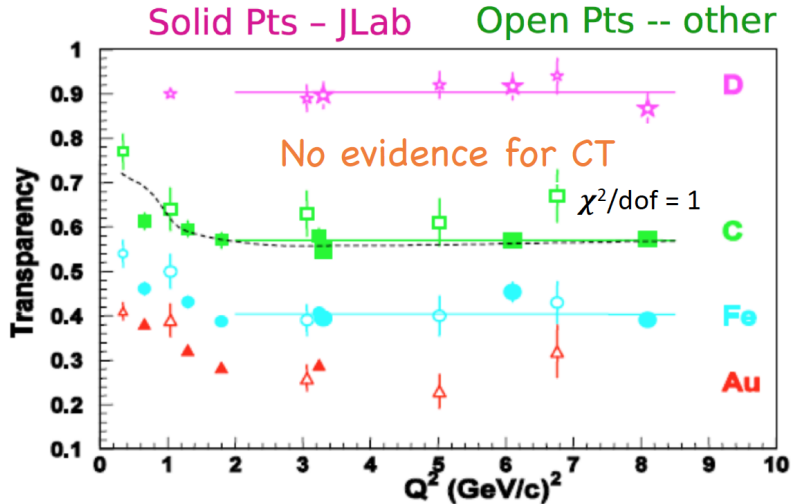


Figure 1: The combined results are shown for  $A(e, e'p)$  searches for CT at MIT-Bates, SLAC, and JLab. A fit is shown that indicates no significant rise consistent with CT. [24–26].

reaction by relating  $t$  to the electron-scattering  $Q^2$ , then the effect observed at BNL has already been ruled out by the experimental results shown in Fig. 1. The most recent result on this topic was performed in a recent Hall C 12 GeV experiment [29] which sought to eliminate the possibility that the increase in transparency observed at BNL is due to the higher incident proton momentum than was observed at JLab during the 6 GeV era. The onset of CT depends both on momentum and energy transfers, affecting the squeezing and freezing, respectively. Since  $A(e, e'p)$  scattering measurements are carried out at  $x_B = 1$  kinematics, they are characterized by lower energy transfers compared to the momentum transfer. It is possible that the 6 GeV era experiments were unable to satisfy the freezing requirement. The results from the most recent experiment in Hall C [29] are shown in Fig. 2, but they do not indicate a rise in CT up to  $Q^2 = 14.2 \text{ GeV}/c^2$  within a 6% uncertainty. It should be noted that these recent results searched for the onset of CT in parallel kinematics (such that the incident struck proton’s momentum is parallel to the electron momentum transfer,  $\vec{q}$ ). The BNL measurements were taken with perpendicular kinematics which in electron scattering is generally dominated by nucleon re-scattering [30–32]. The parallel kinematics in electron scattering are characterized as a regime of already low FSIs.

The recent proton results of [29] reinvigorated the physics community and has since prompted significant ongoing discussion and a re-examination of the CT models. During June of 2021, a workshop dedicated to these efforts was held, titled The Future of Color Transparency and Hadronization Studies at Jefferson Lab and Beyond. Several key ideas have since risen out of this workshop (see a few select topics: [33–37]).

Specifically, [34] is able to explain the lack of observation of the CT onset in the Hall C data as attributable to the Feynman Mechanism. In the Feynman Mechanism, the virtual photon interacts with a single quark that carries a large momentum fraction of the proton such that the proton’s total quark configuration was never in a PLC. A prediction from [33] demonstrates that the onset of CT in protons is expected to occur in “two-stages” where the initial onset  $Q^2$  for the spin-conserving (twist-3) Dirac form factor occurs just above 14  $(\text{GeV}/c)^2$ . The later onset for the spin-flip Pauli (twist-4) form factor occurs at  $Q^2 > 22 \text{ (GeV}/c)^2$ . The theoretical work predicting either the onset of CT in the proton at momentum transfer  $Q^2 > 14 \text{ GeV}^2$  [33] or no PLC formation from the Feynman mechanism [38] is observable through the cross-section dependence on the separation of proton constituents and whether it falls or not with increasing momentum transfer. In the Feynman mechanism vs. CT work [34] and earlier work [39], the cross-section dependence on the

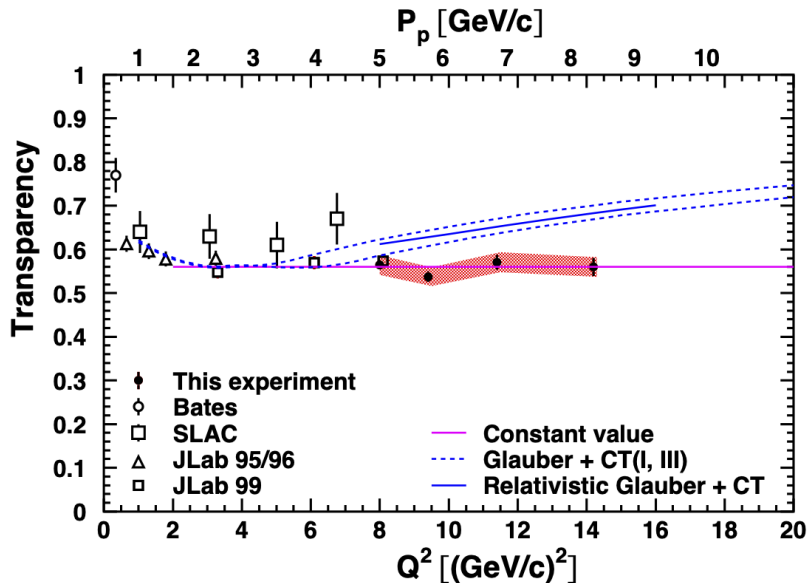


Figure 2: All present carbon electron-scattering results are shown including the latest Hall C measurement [29] indicating no onset in CT up to  $Q^2 = 14.2 \text{ GeV}^2/c^2$ .

square of the transverse separation distance between proton constituents ( $b^2 = \sum_{i < j} (b_i - b_j)^2$ ) is given by  $\lim_{b \rightarrow 0} \sigma(b^2) \propto b^2$ . If  $b^2(Q^2)$  is shown to decrease as  $Q^2$  increases, meaning if the cross-section decreases as  $Q^2$  increases and therefore the transparency  $T$  increases, a PLC is said to be possible/admitted. While holographic light-front QCD (HLFQCD) CT work uses a different variable to define the approach to PLC,  $\mathbf{a}_\perp = \sum_{j=1}^{n-1} x_j \mathbf{b}_{\perp j}$  as the size of the PLC, they are related by a weighting of Bjorken- $x$  [33]. For fractional Bjorken- $x$ , this decreases the cross-sectional dependence as compared to [34, 38] but the overall effect is the same: CT in the proton predicts a decrease in FSI while the Feynman mechanism does not.

A key idea explored by M.Sargsian and W. Boeglin suggests that it is possible to explore the effects of CT in deuterium where the FSI and kinematics are well-understood. While the idea to explore CT in re-scattering kinematics was proposed prior to the 12 GeV upgrade [40], updated predictions from Sargsian that include the constraints from the recent Hall C proton measurement indicate that there is parameter space to observe the signal of CT at  $Q^2 > 12 \text{ (GeV/c)}^2$  as shown in Fig. 3.

Here, the transparency ratio on the vertical axis is taken to be the ratio for high ( $p_r = 400 \text{ MeV/c}$ ) and low ( $p_r = 200 \text{ MeV/c}$ ) recoiling neutron momenta in the  $d(e, e'p)n$  reaction. By taking the ratio of the cross sections for the high and low recoiling nucleons, we see that as we scatter from a PLC (and hence experience less FSI effects), the observed cross section for the high momentum recoiling nucleons decreases as the observed cross section for the low momentum recoiling nucleons increases, and we observe a deviation from traditional Glauber calculations. In Fig. 3, the new prediction to observe such an effect is shown to include the uncertainties and constraints from the recent Hall C measurement. A relative  $Q^2$  dependence of the FSIs could indicate a regime for the onset of CT. This proposal will focus on the use of  $d(e, e'p)n$  as a tool to explore CT in kinematics that were elusive in the previous proton experiments.

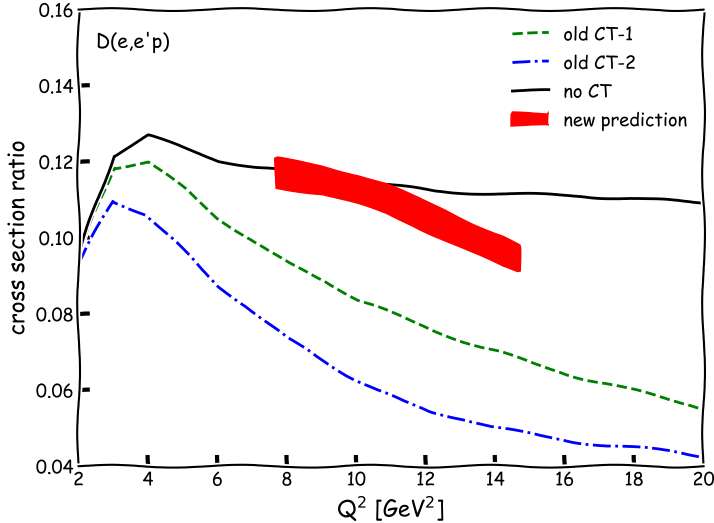


Figure 3: Predictions of cross section ratio  $R = \frac{\sigma(p_r=400\text{MeV}/c)}{\sigma(p_r=200\text{MeV}/c)}$  in the  $d(e, e'p)n$  reaction from [41]. The old CT-1 and 2 curves show the previous calculation including CT effects with expansion parameter  $\Delta M^2=1.1$ , and  $0.7 \text{ GeV}^2$  [40]. They have been ruled out by the new Hall C Carbon results. The red band shows the updated calculation corresponds to the new CT predictions using the constraints and uncertainties of the recent Hall C results. The deviation of this band with respect to black line for the “No CT” prediction indicate the  $Q^2$  region of interest. The “No CT” prediction is calculated using the generalized eikonal approximation. At  $Q^2 = 15 \text{ GeV}^2$ , the new CT prediction deviates from the “No CT” curve by 20%.

## 2 $d(e, e'p)n$

We propose in this experiment to search for the onset signal of CT using deuterium. Deuterium is the simplest target nucleus, and the wave function in collisions is well-described using the generalized eikonal approximation [42, 43]. The kinematics can be precisely chosen such that the inter-nucleon distances of the struck and spectator nucleon lead to well-controlled FSIs [44] and subsequently, enables observations of the formation of the PLC before expansion. The proton knockout reaction in deuterium,  $d(e, e'p)$  is described as:

$$e + d \rightarrow e' + p + n \quad (1)$$

Deuterium is a lighter nucleus compared to the target nuclei used in recent CT experiments and should therefore minimize expansion effects of any observed PLC.

While the inter-nucleon separation is relatively large in deuterium which minimizes deviations with respect to Glauber and should detract from the usefulness of deuterium as a target for CT, there exists an interference between the Born term and the rescattering amplitude of the cross section. The calculation of the cross section shows an increase when the rescattering is included (the square of the rescattering amplitude is dubbed the “double scattering” term) [44], see rescattering in Fig. 4b.

These rescattering effects decrease in the presence of a PLC. In this way, the regions of high FSIs in deuterium may be compared to kinematics with low FSIs with a high degree of sensitivity to PLC formation so that a deviation may be observed as a function of increasing  $Q^2$ . The kinematics of double scattering reactions is optimized where the undetected partner recoil nucleon has a large

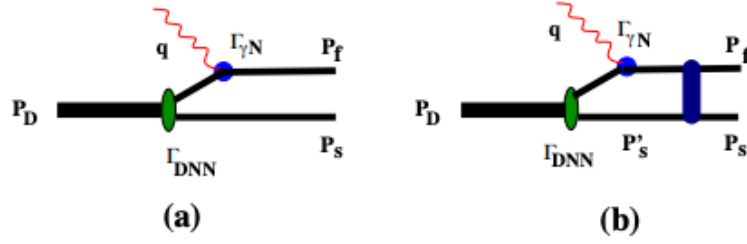


Figure 4: Electron scattering interaction probing deuterium with a) breakup and b) re-scattering effects [41].

perpendicular (with respect to  $\vec{q}$ ) momentum (i.e.  $p_{\perp} \geq 200$  MeV/c for the recoil nucleon). See Fig. 5.

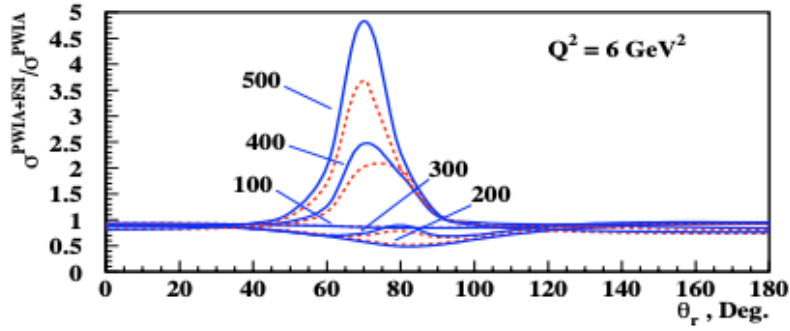


Figure 5: The dependence of the cross section ratio taken with respect to the PWIA on the recoil angle of the neutron ( $\theta_r$ ) for different values of the recoil neutron momenta is shown for  $Q^2 = 6$  (GeV/c)<sup>2</sup> [45].

We will measure the ratios of proton knockout from deuterium where PLC effects are anticipated to be high and compare them to kinematics where the PLC effects are expected to be lower as a function of increasing momentum transfer,  $Q^2$ . Double scattering accesses inter-nucleons distances on the order of 1-2 fm. Access to distances of this small magnitude will enable us to observe PLCs and to help constrain the PLC expansion rate which is anticipated to be rather large due to the lack of recent experimental observation [40]. The larger the momentum of the spectator nucleon, the smaller the inter-nucleon distance and thus, the shorter the distance between the production and re-scattering vertices leading to higher FSI effects. In specific kinematics, the ratio of the measured cross sections between high momentum spectator nucleons and low momentum spectator nucleons,  $R$ , is particularly sensitive to the effects of CT because the numerator, in a regime of high FSIs, will decrease with CT due to an overall reduction in re-scattering whereas the denominator, characterized by low FSIs, will increase. Here we define the missing momentum,  $p_{miss}$  as the momentum of the undetected spectator nucleon:

$$R(Q^2) = \frac{\sigma(p_{miss} \text{ large}; Q^2) \downarrow}{\sigma(p_{miss} \text{ small}; Q^2) \uparrow} \quad (2)$$

Here,  $R$  is expected to decrease with increasing  $Q^2$  in the presence of PLCs. The regime where  $p_{miss}$  is large is chosen in the range of 300 – 600 MeV/c where double scattering dominates. Also, the reconstructed angle of the recoiling nucleon should be in the range of 60–90° where FSI effects deviate most from PWIA calculation. The increase in the cross section is shown in data from [46] in Fig. 6.

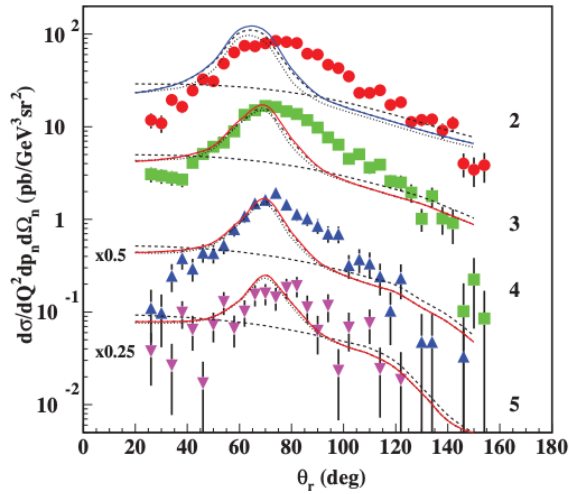


Figure 6: Data from [46] shows the dependence of the differential cross section on the recoil neutron angle and momentum where the momentum of the recoil neutron for these data is restricted to be between 400–600 MeV/ $c$ . The dashed line shows the PWIA calculation while the other lines show calculations that include PWIA and other FSI effects [45]. The different colors of data points correspond to different  $Q^2$  ranging from 2–5 (GeV/ $c$ )<sup>2</sup>, increasing from top to bottom.

In the regime where  $p_{miss}$  is small, we are interested in nucleons with momenta  $< 200$  MeV/ $c$  where Glauber screening is expected to play a large effect. Previous data from [46] shows the measured cross sections for the lower momenta recoiling neutrons in Fig. 7. Our ratio will be taken with respect to data and will be compared to ratios constructed from theory. Note that this approach is unique from previous electron scattering proton knockout CT experiments which compare data directly to theoretical calculations.

The signal in both the regions of low and high  $p_{miss}$  is optimized where the light cone momentum fraction of the nucleus carried by the recoil nucleon,  $\alpha$ , is approximately 1 (i.e.  $\alpha$  is defined as  $(E_n - p_n \cos \theta_{\gamma n})/m_n$  in terms of the final state spectator nucleon energy, momentum, mass, and angle). The model we use to study the deuteron and make such comparisons is from AV18 for the nucleon momentum distribution. We further make comparisons in terms of the Plane Wave Impulse Approximation (PWIA) and the FSIs.

### 3 The Proposed Measurement

We propose to measure the onset of CT in  $d(e, e'p)n$  by detecting the electron and proton in coincidence in Hall C from electron scattering on a deuterium target. We will construct ratios of the protons detected with high missing momenta (300 – 600 MeV/ $c$ ) to those having low missing momenta (50 – 150 MeV/ $c$ ) as a function of  $Q^2$ . We will explore a range of  $Q^2$  that overlaps with the previous E12-06-107 experiment which was taken in parallel kinematics. By the time of this experimental running, we expect to receive 11 GeV of beam in Hall C. This, together with the full momentum capabilities of the Hall C spectrometers, will extend our measured  $Q^2$  up to 15 (GeV/ $c$ )<sup>2</sup>.

This measurement will increase our sensitivity for observing protons in a PLC. We will measure the ratio of experimental quantities with respect to experimental quantities, and we will compare this ratio with theory ratios taken with respect to theory. This is a different approach to the previous electron-scattering CT experiments which measure the ratios of experimental quantities direct with



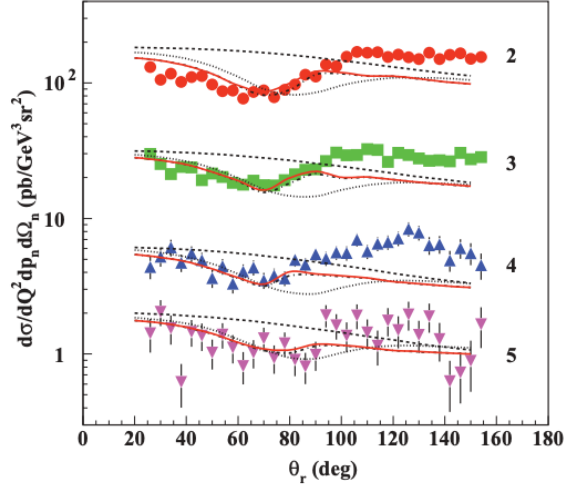


Figure 7: Data from [46] shows the dependence of the differential cross section on the recoil neutron angle and momentum where the momentum of the recoil neutron for these data is restricted to be between 200–300 MeV/c. The dashed line shows the PWIA calculation while the other lines show calculations that include PWIA and other FSI effects [45]. The different colors of data points correspond to different  $Q^2$  ranging from 2–5 (GeV/c) $^2$ , increasing from top to bottom.

theory, and it reduces our overall systematic uncertainties. Uniquely, this experiment will measure proton knockout in a regime with high FSI contributions ( $\alpha \approx 1$ ).

We plan to use a 25 cm liquid deuterium target (5% radiation length) to receive beam at 80  $\mu$ A for a luminosity per proton of  $6.23 \times 10^{38} \text{ A}^{-1} \text{ cm}^{-2} \text{ s}^{-1}$ . The 25 cm target will significantly increase our statistics compared to the standard Hall C 10 cm target, but requires more cooling power, which will be possible after the ESR-2 upgrade. We use an aluminum dummy target for background target cell subtraction. The spectrometer detectors will be used in their standard configurations.

### 3.1 Kinematics

While many of the previous electron scattering CT experiments on the proton have utilized parallel kinematics to reduce FSIs, here we employ perpendicular kinematics to increase FSIs and to measure CT in re-scattering reactions in an effort to improve our sensitivity to the formation of PLCs. We will use five kinematics settings to cover  $Q^2$  from 8 to 15 GeV $^2$  (see Table 1). At each setting, the HMS will detect the scattered electrons at the quasi-elastic peak, while high-momentum struck protons will be measured in the SHMS. The SHMS momentum is centered at  $P_{miss} = -200 \text{ GeV}/c$  to cover both the low and high  $P_{miss}$  regions simultaneously. We focus on the negative  $P_{miss}$  (backward kinematics where the struck proton goes backward with respect to  $\vec{q}$ ) to get more counts and fewer background pions. We calculated the ratio of (PWIA+FSI)/PWIA as a function of the recoiling neutron angle for each kinematic setting in Fig. 8. The impact of the FSI is slightly reduced with increasing  $Q^2$ , but it still shows a strong enhancement at  $P_{miss}$  between 300 to 600 MeV/c, and a suppression at  $50 < P_{miss} < 150 \text{ MeV}/c$ .

The missing momentum resolution is shown in Fig. 9 for the  $Q^2 = 14 \text{ (GeV}/c)^2$  setting and is shown to be approximately 7 MeV. This resolution is consistent with that observed in the previous CT Hall C measurement [29]. Furthermore, the missing mass is reconstructed at each kinematic setting. In our simulations, we reconstruct the missing mass of the neutron with and without radiative effects. We optimize our rate and kinematic studies with a cut on the neutron mass

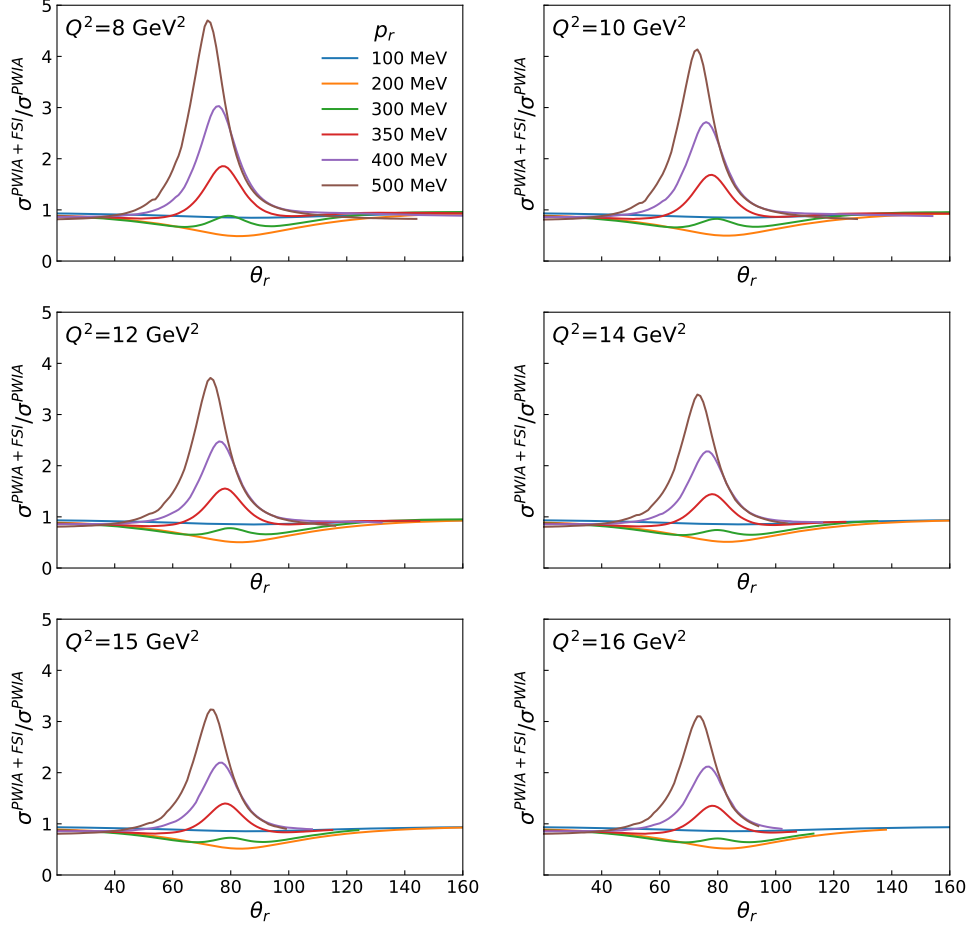


Figure 8: The dependence of the cross section ratio taken with respect to the PWIA on the recoil angle of the neutron with respect to  $\vec{q}$  ( $\theta_{rq}$ ) for different values of the recoil neutron momenta is shown for  $Q^2 = 8$  to  $16$  ( $\text{GeV}/c$ ) $^2$ .

$\pm 0.1$  GeV. The effect of the missing mass cut on the reconstructed neutron mass is shown in Fig. 11. This cut is essential to ensure that we have adequately reconstructed the recoiling nucleon.

### 3.2 Expected Rates

Kinematics and rate studies are done with the Hall C SIMC Monte-Carlo simulation package [47]. The deuteron cross section is calculated with the CC1 off-shell prescription [48] and the AV18 deuteron momentum distribution [49]. The effects of FSI are included by following the same calculation in [45]. No charge exchange are considered in the rate estimation. The expected coincidence rates per hour are integrated over two  $P_{miss}$  region at each  $Q^2$ , see Table 2. The overall times for run-

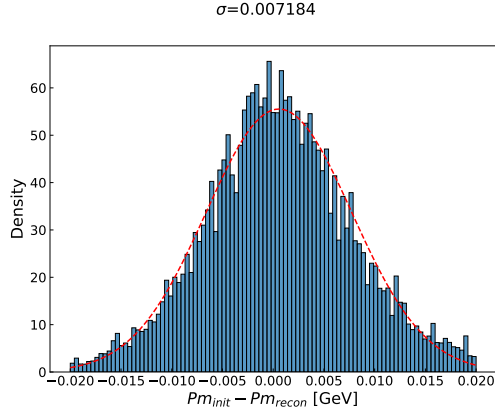


Figure 9: The  $P_m$  resolution at  $Q^2 = 14 \text{ (GeV}/c)^2$  is about 7 MeV.

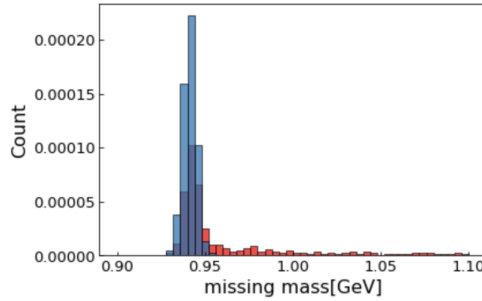


Figure 10: The missing mass from SIMC with(red) and without(blue) radiative effect at  $Q^2 = 14 \text{ (GeV}/c)^2$  both peak at neutron mass.

Table 1: Proposed Kinematics

Kinematics	$Q^2$	$P_e \text{ (GeV}/c)$	$\theta_e \text{ (deg)}$	$P_p \text{ (GeV}/c)$	$\theta_p \text{ (deg)}$
1	8.046	6.713	19.000	5.121	27.380
2	9.958	5.694	23.000	6.154	22.972
3	11.941	4.637	28.000	7.222	19.073
4	14.026	3.525	35.000	8.341	15.363
5	15.127	2.939	40.000	8.931	13.461

ning on each target at each kinematic setting are shown for 1000 coincidence counts (corresponding to statistical uncertainty of approximately 3%) in the high  $P_{miss}$  region (kinematics b). Kinematical settings 1 and 2 are scaled to match statistics from the recent Hall C CT experiment, that is, 5k and 2k events respectively. An overall efficiency factor of 0.8 is applied to all time estimations and is estimated from the measured experimental inefficiency in the recent Hall C CT measurement.

The total measurement times shown in Table 2 are given in PAC days. Additional running on the aluminum dummy cell for the window background subtraction will require approximately two percent of the beam time used for the full target (adding an additional 2 days of beam in total). Configuration changes and calibration runs are expected to take 2 more PAC days. The total time requested for this experiment is approximately 95 days.

Q<sup>2</sup>=15 GeV<sup>2</sup>, e\_angle=40 degree

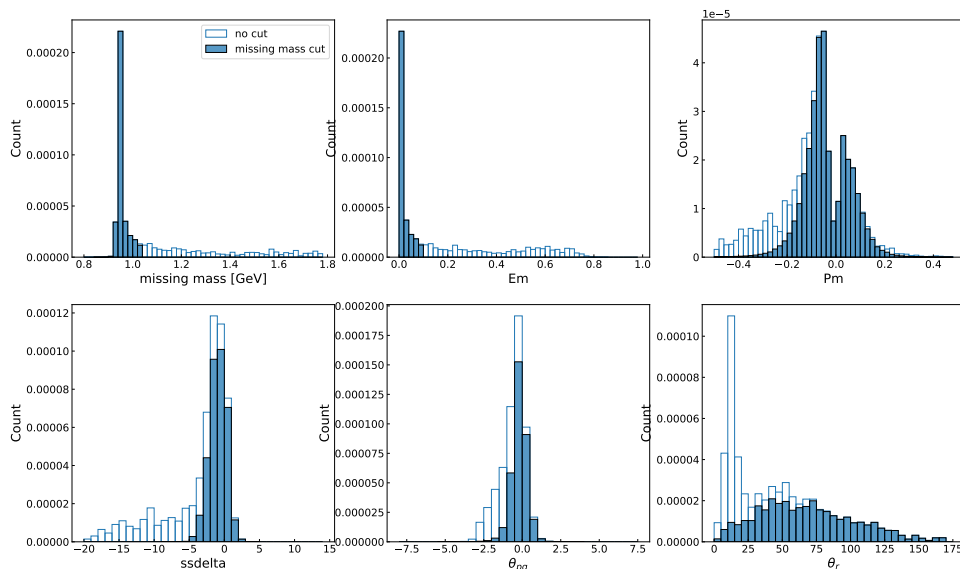


Figure 11: Kinematics variables from SIMC before (non-filled) or after (filled, blue) a missing mass cut of neutron mass $\pm 0.1$  GeV at  $Q^2 = 15$  (GeV/c)<sup>2</sup>.

Table 2: The expected  $ep$  coincidence rates per hour are shown for each kinematics at two missing momentum ranges, a: 50-150 MeV, b: 300-600 MeV, along with their  $P_m, \theta_r, Q^2$  in weighted average. ‘‘PAC days’’ shows the time needed for each high  $P_m$  region (b) to accumulate 1000 counts with an efficiency factor of 80% (except for settings 1 and 2 which will detect 5k and 2k events in this regime). SIMC with radiative effects included is used for this estimation, assuming 80  $\mu$ A beam on a 25cm liquid deuterium target.

	<b>Kinematics</b>	$P_m$	$\theta_r$	$Q^2$	<b>Rate/hour</b>	<b>PAC days</b>
1	a	0.08	79.06	7.49	5690.81	1.5
	b	0.41	73.33	7.88	149.04	
2	a	0.08	77.15	9.52	1536.20	3.0
	b	0.41	74.44	9.77	36.47	
3	a	0.08	77.40	11.62	413.28	5.7
	b	0.41	75.46	11.70	9.16	
4	a	0.09	77.28	13.76	93.63	25.1
	b	0.40	75.95	13.74	2.07	
5	a	0.09	78.73	14.94	36.63	55.9
	b	0.40	75.72	14.83	0.93	

### 3.3 Systematics

We assume the measured systematics from the previous Hall C measurement of 4% as an estimate of what to expect in this experiment. We will use ratios which will reduce some of the magnitude of the systematics. The largest systematics from the Hall C measurement were on the spectrometer acceptance (2.6%) which we expect to reduce from better knowledge of the spectrometers and with the use of experimental transparency ratios taken at the same kinematics. The next largest sources

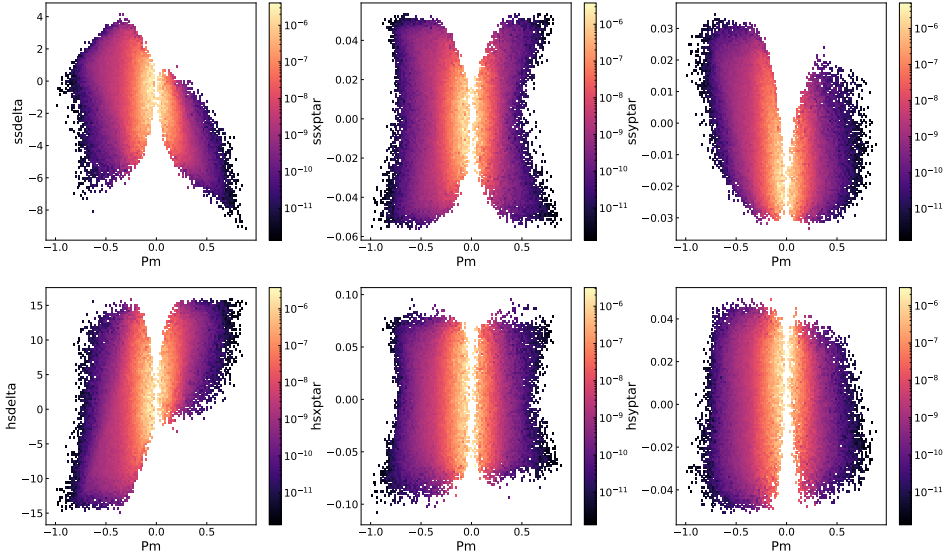


Figure 12: SHMS and HMS target variables from SIMC with respect to  $P_{miss}$  at  $Q^2 = 14 \text{ (GeV/c)}^2$  after the missing mass cut.

of uncertainty were on the knowledge of the fundamental  $ep$  elastic cross section (1.8%) and the proton absorption in materials between the target and detector (1.2%). Both of these effects will be minimized as systematic contributions through the use of experimental ratios.

## 4 Complementary Experiments at JLab

Experiments in the JLab 6 GeV era observed the onset of CT in mesons. Hall C observed the onset of CT in pion electroproduction in E01-107 in the range of  $Q^2 = 1\text{-}5 \text{ GeV}/c^2$  [13] [50] on  $^{12}\text{C}$ ,  $^{27}\text{Al}$ ,  $^{63}\text{Cu}$ , and  $^{197}\text{Au}$  targets. CLAS experiment E02-110 measured the onset in rho electroproduction on  $^{12}\text{C}$  and  $^{56}\text{Fe}$  targets at  $Q^2$  between 0.8-2.4  $\text{GeV}/c^2$  [14]. The CLAS experiment E12-06-106 [51] further investigates the nuclear target and  $Q^2$  dependence of CT in rho meson electroproduction up to  $Q^2 = 5.5 \text{ GeV}/c^2$ . The onset of CT in mesons confirms the presence of hadrons in point-like configurations (PLCs) and further motivates the search for baryons in such configurations. The  $Q^2$  at which CT begins in mesons versus baryons is unknown as well as the nucleus  $A$ -dependence, but the measurement of the onset in baryons will elucidate information about PLC expansion times and effects in nuclear physics.

After the 12 GeV upgrade, E12-06-107 [52] ruled out the onset of CT in  $A(e, e'p)$  reactions up to  $Q^2 = 14.2 \text{ GeV}/c^2$  in parallel kinematics. No other experiment will have measured the CT effect in our proposed kinematics, but it should be noted that this  $d(e, e'p)$  strategy has been a key approach to observing CT that was even included in motivation for the 12 GeV upgrade [40]. The onset of CT is a requirement for the validity of the QCD factorization theorem [53] for exclusive meson production in DIS (a critical experimental and theoretical effort at JLab).

We propose 95 days of beam running in Hall C with a 11 GeV electron beam at  $80 \mu\text{A}$  to measure the  $d(e, e'p)$  reaction in the standard HMS and SHMS spectrometers in coincidence. This

measurement will extend the previous measurements that did not observe the onset of CT in protons in parallel kinematics, but we will search for the onset of CT in transverse kinematics characterized as having higher FSIs and may prove to be more sensitive to observing the onset of PLCs.

## References

- [1] S. J. Brodsky and G. R. Farrar, “Scaling Laws for Large Momentum Transfer Processes,” *Phys. Rev. D*, vol. 11, p. 1309, 1975.
- [2] S. J. Brodsky, L. Frankfurt, J. F. Gunion, A. H. Mueller, and M. Strikman, “Diffractive lepto-production of vector mesons in QCD,” *Phys. Rev. D*, vol. 50, pp. 3134–3144, 1994.
- [3] J. C. Collins, L. Frankfurt, and M. Strikman, “Factorization for hard exclusive electroproduction of mesons in QCD,” *Phys. Rev. D*, vol. 56, pp. 2982–3006, 1997.
- [4] L. L. Frankfurt, P. V. Pobylitsa, M. V. Polyakov, and M. Strikman, “Hard exclusive pseudoscalar meson electroproduction and spin structure of a nucleon,” *Phys. Rev. D*, vol. 60, p. 014010, 1999.
- [5] M. Diehl, T. Gousset, B. Pire, and O. Teryaev, “Probing partonic structure in  $\gamma^* \gamma \rightarrow \pi \pi$  near threshold,” *Phys. Rev. Lett.*, vol. 81, pp. 1782–1785, 1998.
- [6] X.-D. Ji, “Deeply virtual Compton scattering,” *Phys. Rev. D*, vol. 55, pp. 7114–7125, 1997.
- [7] A. V. Radyushkin, “Nonforward parton distributions,” *Phys. Rev. D*, vol. 56, pp. 5524–5557, 1997.
- [8] L. L. Frankfurt and M. I. Strikman, “Hard Nuclear Processes and Microscopic Nuclear Structure,” *Phys. Rept.*, vol. 160, pp. 235–427, 1988.
- [9] B. Jennings and G. Miller, “Color transparency: The Wherefore and the Why,” *Phys. Rev. D*, vol. 44, pp. 692–703, 1991.
- [10] G. Miller, private e-mail communication.
- [11] O. Hen, G. A. Miller, E. Piassetzky, and L. B. Weinstein, “Nucleon-Nucleon Correlations, Short-lived Excitations, and the Quarks Within,” *Rev. Mod. Phys.*, vol. 89, no. 4, p. 045002, 2017.
- [12] B. Blaettel, G. Baym, L. L. Frankfurt, and M. Strikman, “How transparent are hadrons to pions?,” *Phys. Rev. Lett.*, vol. 70, pp. 896–899, 1993.
- [13] B. Clasie *et al.*, “Measurement of Nuclear Transparency for the  $A(e, e' \pi^+)$  Reaction,” *Phys. Rev. Lett.*, vol. 99, p. 242502, 2007.
- [14] L. El Fassi *et al.*, “Evidence for the onset of color transparency in  $\rho^0$  electroproduction off nuclei,” *Phys. Lett. B*, vol. 712, pp. 326–330, 2012.
- [15] L. Frankfurt, G. A. Miller, and M. Strikman, “Color Transparency in Semi-Inclusive Electroproduction of rho Mesons,” *Phys. Rev. C*, vol. 78, p. 015208, 2008.
- [16] K. Gallmeister, M. Kaskulov, and U. Mosel, “Color transparency in hadronic attenuation of  $\rho^0$  mesons,” *Phys. Rev. C*, vol. 83, p. 015201, 2011.
- [17] A. S. Carroll *et al.*, “Nuclear Transparency to Large Angle  $pp$  Elastic Scattering,” *Phys. Rev. Lett.*, vol. 61, pp. 1698–1701, 1988.

- [18] I. Mardor *et al.*, “Nuclear transparency in large momentum transfer quasielastic scattering,” *Phys. Rev. Lett.*, vol. 81, pp. 5085–5088, 1998.
- [19] A. Leksanov *et al.*, “Energy dependence of nuclear transparency in  $C(p, 2p)$  scattering,” *Phys. Rev. Lett.*, vol. 87, p. 212301, 2001.
- [20] J. Aclander *et al.*, “Nuclear transparency in  $90^\circ_{\text{c.m.}}$  quasielastic  $A(p, 2p)$  reactions,” *Phys. Rev. C*, vol. 70, p. 015208, 2004.
- [21] B. Kundu, J. Samuelsson, P. Jain, and J. P. Ralston, “Perturbative color transparency in electroproduction experiments,” *Phys. Rev. D*, vol. 62, p. 113009, 2000.
- [22] J. P. Ralston and B. Pire, “Quantum chromotransparency,” *Phys. Rev. Lett.*, vol. 65, pp. 2343–2346, 1990.
- [23] S. J. Brodsky, I. Schmidt, and G. F. de Téramond, “Nuclear-bound quarkonium,” *Phys. Rev. Lett.*, vol. 64, pp. 1011–1014, Feb 1990.
- [24] D. Abbott *et al.*, “Quasifree  $(e, e'p)$  reactions and proton propagation in nuclei,” *Phys. Rev. Lett.*, vol. 80, pp. 5072–5076, 1998.
- [25] N. Makins *et al.*, “Momentum transfer dependence of nuclear transparency from the quasielastic  $^{12}\text{C}(e, e'p)$  reaction,” *Phys. Rev. Lett.*, vol. 72, pp. 1986–1989, 1994.
- [26] K. Garrow *et al.*, “Nuclear transparency from quasielastic  $A(e, e'p)$  reactions up to  $Q^2 = 8.1(\text{GeV}/c)^2$ ,” *Phys. Rev. C*, vol. 66, p. 044613, 2002.
- [27] T. G. O’Neill *et al.*, “A-dependence of nuclear transparency in quasielastic  $A(e, e'p)$  at high  $Q^2$ ,” *Phys. Lett. B*, vol. 351, pp. 87–92, 1995.
- [28] S. Frullani and J. Mougey, “Single-particle properties of nuclei through  $(e, e'p)$  reactions,” *Advances in Nuclear Physics*, vol. 14, 1984.
- [29] D. Bhetuwal, J. Matter, H. Szumila-Vance, M. L. Kabir, D. Dutta, R. Ent, *et al.*, “Ruling out color transparency in quasielastic  $^{12}\text{C}(e, e'p)$  up to  $Q^2$  of 14.2  $(\text{GeV}/c)^2$ ,” *Phys. Rev. Lett.*, vol. 126, p. 082301, Feb 2021.
- [30] C. Barbieri and L. Lapikas, “Effects of rescattering in  $(e, e\text{-prime } p)$  reactions within a semiclassical model,” *Phys. Rev. C*, vol. 70, p. 054612, 2004.
- [31] D. Rohe *et al.*, “Nuclear transparency from quasielastic C-12  $(e, e\text{-prime } p)$ ,” *Phys. Rev. C*, vol. 72, p. 054602, 2005.
- [32] D. Rohe *et al.*, “Correlated strength in nuclear spectral function,” *Phys. Rev. Lett.*, vol. 93, p. 182501, 2004.
- [33] S. J. Brodsky and G. F. de Teramond, “Onset of color transparency in holographic light-front qcd,” 2022.
- [34] G. A. Miller, “Color transparency and light front holographic qcd,” 2022.
- [35] P. Jain, B. Pire, and J. P. Ralston, “The status and future of color transparency and nuclear filtering,” 2022.
- [36] G. M. Huber, W. B. Li, W. Cosyn, and B. Pire, “u-channel color transparency observables,” 2022.

- [37] K. Gallmeister and U. Mosel, “Hadronization and color transparency,” 2022.
- [38] O. Caplow-Munro and G. A. Miller, “Color transparency and the proton form factor: Evidence for the Feynman mechanism,” *Phys. Rev. C*, vol. 104, no. 1, p. L012201, 2021.
- [39] L. Frankfurt, G. A. Miller, and M. Strikman, “Precocious dominance of point-like configurations in hadronic form-factors,” *Nucl. Phys. A*, vol. 555, pp. 752–764, 1993.
- [40] M. M. Sargsian, J. Arrington, W. Bertozzi, W. Boeglin, C. E. Carlson, D. B. Day, L. L. Frankfurt, K. Egiyan, R. Ent, S. Gilad, K. Griffioen, D. W. Higinbotham, S. Kuhn, W. Melnitchouk, G. A. Miller, E. Piasetzky, S. Stepanyan, M. I. Strikman, and L. B. Weinstein, “Hadrons in the nuclear medium,” *Journal of Physics G: Nuclear and Particle Physics*, vol. 29, pp. R1–R45, feb 2003.
- [41] W. Boeglin and M. Sargsian, “Color transparency and hadronization studies with the deuteron,” 2021.
- [42] P. Capel, “The eikonal model of reactions involving exotic nuclei; Roy Glauber’s legacy in today’s nuclear physics,” *SciPost Phys. Proc.*, vol. 3, p. 017, 2020.
- [43] M. M. Sargsian, T. V. Abrahamyan, M. I. Strikman, and L. L. Frankfurt, “Exclusive electrodisintegration of He-3 at high  $Q^{*2}$ . I. Generalized eikonal approximation,” *Phys. Rev. C*, vol. 71, p. 044614, 2005.
- [44] L. L. Frankfurt, W. R. Greenberg, G. A. Miller, M. M. Sargsian, and M. I. Strikman, “Color transparency effects in electron deuteron interactions at intermediate  $Q^{*2}$ ,” *Z. Phys. A*, vol. 352, pp. 97–113, 1995.
- [45] M. M. Sargsian, “Large  $Q^2$  Electrodisintegration of the Deuteron in Virtual Nucleon Approximation,” *Phys. Rev. C*, vol. 82, p. 014612, 2010.
- [46] K. S. Egiyan *et al.*, “Experimental study of exclusive  ${}^2\text{H}(e, e'p)n$  reaction mechanisms at high  $Q^2$ ,” *Phys. Rev. Lett.*, vol. 98, p. 262502, Jun 2007.
- [47] “Simc monte carlo.”
- [48] T. De Forest, “Off-Shell electron Nucleon Cross-Sections. The Impulse Approximation,” *Nucl. Phys.*, vol. A392, pp. 232–248, 1983.
- [49] R. B. Wiringa, R. Schiavilla, S. C. Pieper, and J. Carlson, “Nucleon and nucleon-pair momentum distributions in  $a \leq 12$  nuclei,” *Phys. Rev. C*, vol. 89, p. 024305, Feb 2014.
- [50] X. Qian *et al.*, “Experimental study of the  $A(e, e'\pi^+)$  Reaction on  ${}^1\text{H}$ ,  ${}^2\text{H}$ ,  ${}^{12}\text{C}$ ,  ${}^{27}\text{Al}$ ,  ${}^{63}\text{Cu}$  and  ${}^{197}\text{Au}$ ,” *Phys. Rev. C*, vol. 81, p. 055209, 2010.
- [51] K. Hafidi *et al.*, “Jefferson Lab 12 GeV experiment E12-06-106.” <https://misportal.jlab.org/mis/physics/experiments/viewProposal.cfm?paperId=685>.
- [52] D. Dutta *et al.*, “Jefferson Lab 12 GeV experiment E12-06-107.” <https://misportal.jlab.org/mis/physics/experiments/viewProposal.cfm?paperId=686>.
- [53] M. Strikman, “QCD factorization theorems for DIS exclusive processes and inclusive diffraction: New probes of hadrons and nuclei,” *Nucl. Phys. A*, vol. 663, pp. 64–73, 2000.